Retrieval of computer generated holograms projected onto liquid crystal - photoconducting polymer syste

Andrzej Miniewicz [a], Jaroslaw Mysliwiec[a], Lukasz Gryga[a], and François Kajzar[b]

[a] Institute of Physical and Theoretical Chemistry, Wroclaw University of Technology, 50-370 Wroclaw, Poland
[b] CEA Saclay, DRT/LITEN/DECS/SE2M, Bat 451 F91191 Gif Sur Yvette, France

ABSTRACT

Simple liquid crystal panel equipped with a polymeric photoconducting layer can be used for displaying dynamic holographic images. It is sufficient to compute the hologram of the object and reconstruct the wavefield optically. This can be done by projection of the binary hologram onto liquid crystal panel with the help of standard video-projector Illumination of the photoconducting polymeric layer by a white light interferogram leads to tiny molecula rearrangements within the bulk of the liquid crystal layer which form a refractive index grating. They occur as a result of spatially modulated electric space charge field produced in a polymer. Short holographic films displayed at video-rates are achievable with the system based on PVK:TNF polymer and plana nematic liquid crystal mixture. The underlying electrical and optical processes as well as characteristics, performances and limitations of the system are discussed.

Keywords: optically addressed liquid crystalline spatial light modulators, real-time holography, optical retrieval of binary holograms, transient gratings, refractive index gratings, nematic liquid crystal, poly(vinyl carbazole) photoconducting polymer

1. INTRODUCTION

Future commercial visualization systems as well as many scientific implementations (e.g. holographic interferometry [1] or holographic optical tweezers [2]) will require holographic projection i.e. a three-dimensional (3-D) image exhibiting all the effects of perspective and depth of focus [3]. A hologram usually recorded with two coherent lase beams on a flat surface contains information about the entire (3-D) wavefield in the form of microinterferences. In classic holography these microinterferences are mapped into absorption modulations of a high spatial resolution photographic plate. In modern approach the refractive index changes are preferred as they allow for higher light diffraction efficiency and lack of light attenuation (initially inorganic photorefractive crystals met these requirements [4], later on novel materials were developed like photorefractive polymers [5-8], liquid crystals (LCs) [9-14] including polymer-dispersed liquid crystals (PDLCs) [15,16] or polymer-stabilized liquid crystals (PSLCs) [17-19] and photochromic polymers [20-24]. The dynamic (or real-time) holography requires the fully reversible photosensitive material lacking any post-processing. The development of computers and liquid crystalline spatial light modulators enabled transferring either the recording process or the reconstruction into the computer [25]. In this communication we discuss the case of computer-generated holograms and their optical reconstruction [26-28] using optically addressed liquid crystalline spatial light modulators OA LC SLM. To accomplish this, one usually requires a digital light processing (DLP) device i.e. a high-resolution computer-controlled real-time spatial light modulator. The most frequently used are reflection or transmission type electrically addressed liquid crystalline spatial light modulators (EA LC SLM) [29-31] or reflective digital micro-mirror devices (DMD) [32]. Advantage of their usage is a full electronic control over optical state of any pixel within a matrix, however the necessity of discrete structure limits thei application because of unwanted light diffraction on periodic structure of pixels.

2. FUNCTIONING PRINCIPLES OF OPTICALLY ADDRESSED LIQUID CRYSTAL SPATIAL LIGHT MODULATOR

Liquid crystals are birefringent and they therefore influence the state of polarization of light beams. This interaction is described by the Jones calculus [33]. In a birefringent material, each eigenwave sees a different refractive index and will propagate at a different speed. This leads to a phase retardation between the two eigenwaves which is dependent on the thickness of the birefringent material and the wavelength of the light. The point is to construct a device (retardation plate) with light illumination intensity dependent retardation. This could be done employing photorefractive properties of liquid crystals. Liquid crystals and among them speciall nematics do not exhibit photorefractive effect in a classic sense (restricted to photoconducting and nonlinear optical materials) as they are centrosymmetric, and in consequence do not show electro-optic activity. However, photorefractive-like properties of nematics are well-recognized and it is widely accepted that light could impose molecular reorientation through different mechanisms: like thermal, dye-induced or surface induced reorientations [34-38]. In this work we used a designed and fabricated by us LC cell able to perform tasks of OA LC SLM [39,40]. The pure nematic liquid crystal mixture is confined in a planar cell (10 μm in thickness) with transparent ITO electrodes and orienting coatings. One of them was made of a spin-coated (100 nm thick) photoconductive poly(N-vinyl carbazole) PVK doped with 2,4,7-trinitrofluorenone (TNF) or 2,4,7-trinitro-9-fluorenilidene-malononitrile (TNFDM) to induce its sensitivity in the visible. PVK:TNF or PVK:TNFDM 12:1 mixtures were dissolved in $CHCl_3$ and the layer was spin-coated at 2500 rpm directly on ITO covered glass plates which were dried at 100^oC for 5 hours after deposition. Both polymeric layers photoconductive and that made of polyimide (100 nm thick on average) were uniaxially brushed. A schematic structure of the hybrid photoconducting polymer - liquid crystal device developed by us is shown in Fig. 1.
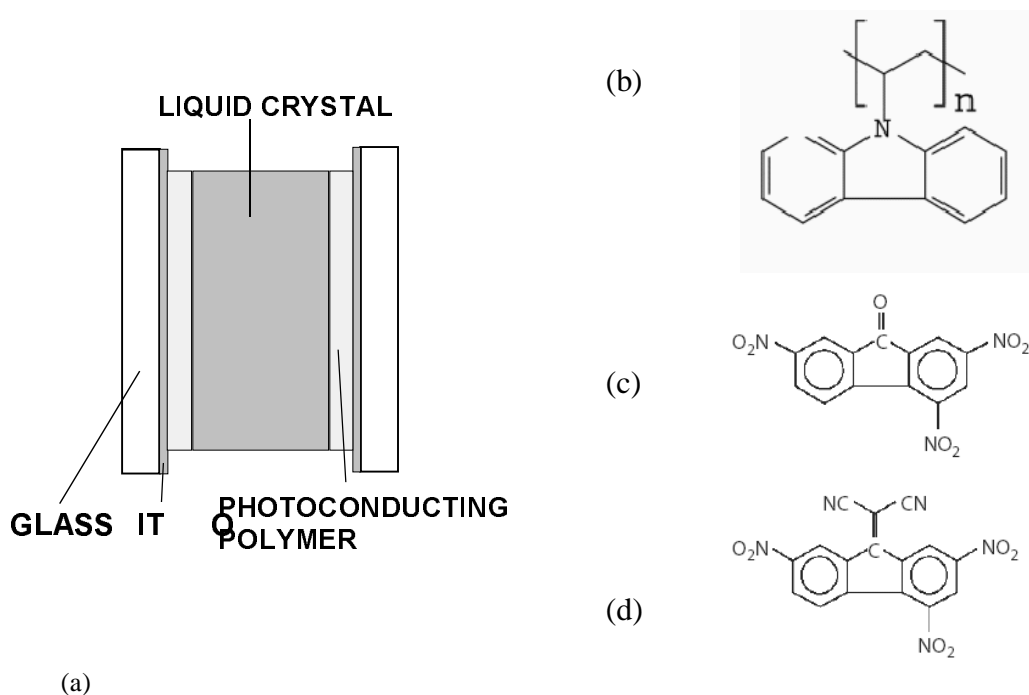

Figure 1. A schematic structure of the liquid crystal panel used in the present studies. The thicknesses of the respective layers are given in the text. The external dc voltage was supplied to the panel with the help of thin wires attached to the ITO conducting layers (a). Chemical formulae of PVK (b), TNF (c) and TNFDM (d).

The layers showed optical uniformity over the whole display area (10 cm x 5 cm) and small absorption of 8 - 14 cm^{-1} at charge transfer CT absorption band centered at 550 nm. Illumination at both 514 nm and 632.8 nm have led to photogeneration of charge carriers in the system. The plates were sandwiched in parallel to each other with the use of a 10 μm polyester spacer and keeping the parallel rubbing direction. The cells were filled by a capillary action with a multicomponent nematic liquid crystal mixture E7 (Merck KGaA, Darmstadt, Germany) and showed homogenous alignment. Such a LC composition at room temperature is characterized by a positive static dielectric anisotrop $\Delta\varepsilon$ = +13.8, birefringence Δn = 0.2253 at 589 nm (n_e = 1.7464, n_o = 1.5211) and viscosity γ = 39 mm^{2}s^{-1}. The dc voltage within a range 0 - 20 V was sufficient to change the director orientation (average alignment direction of the long molecular axes of nematic liquid crystal) from homogenous (planar) to nearly homeotropic (perpendicular to glass plates). The effect of dc alignment was checked by light retardation studies in separate measurements using Mach-Zehnder interferometer.
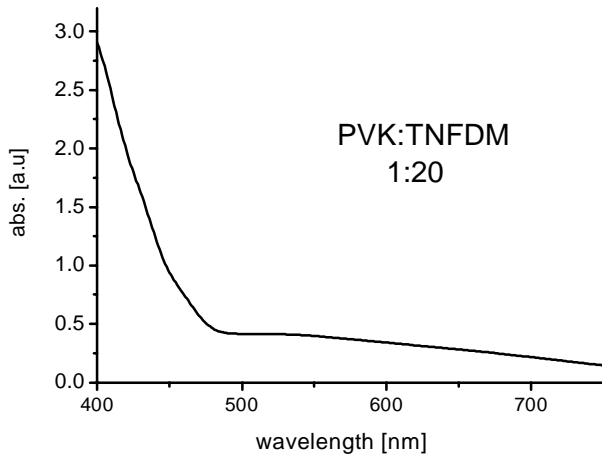

Fig. 2. Absorption spectrum of a PVK:TNFDM thin layer deposited on ITO glass. The charge transfer transition band between carbazole unit and 2,4,7-trinitro-9-fluorenilidene-malononitrile (TNFDM) molecule is visible with maximum around 570 nm.

Placing the modulator in one arm of a Mach-Zehnder interferometer we were able to address it with a 514.5 nm light passing through electrically addressed spatial light modulator 640x480 pixels. Light induced reorientation of molecules allowed directly observe the phase changes seen by extraordinary polarized plane wave of 632.8 nm wavelength feeding the interferometer. An example of such type observation is shown in Fig. 3.

Fig. 3. Example of optical addressing of liquid crystalline panel placed into one arm of Mach- Zehnder interferometer. From left to right are shown: object image superimposed onto 514.5 nm expanded laser beam, phase contrast due to interference of image bearing beam 632.8 nm with reference beam of interferometer and a phase map. The phase difference seen in this case was 2 π and the phase nonuniformit exceeded π/4 mostly due to panel misalignment.

Spatiall modulated light I (x,y) incident on the biased LC cell induces charge carrie photogeneration process with photoconductive sensitivity depending on light intensity and a biasing electric field within a polymeric laye E_p: $\sigma / I = e\alpha\mu(E_p)\tau\Phi(E_p)/h\nu$, where e is the electron charge, α the absorption coefficient, hν the photon energy, τ the life-time of the photocarrier and $\mu(E_p)$ the carrier mobility. The efficiency of photogeneration $\Phi(E_p)$ as follows from the Onsager theory [41] is a function of local electric field E_p. The space charge field E_{sc} (t) arising due to photoexcitation together with the externally applied dc electric field exert charge carrier drift through the layer thickness. In the PVK:TNF the more mobile holes are easily moved by the electric field from the photogeneration place leaving the less mobile electrons at thei photogeneration sites. Holes are neutralized on negatively biased ITO front electrode living distribution of much slower electrons in polymeric layer. Under constant light illumination the charge densit distribution is established which is converted into respective changes of surface potential. In the process also ionic transport through the LC layer is important as it tends to compensate an excess charge. The actual electric field acting on LC molecules E_{LC} is dependent on distance form the polymeric layer (z) and diminishes toward the center of LC layer due to the Debye screening effect. The electric field distribution within LC layer changes extraordinary effective index of refraction $\Delta n_e(x,y,z)$ in its bulk:

$$\left\langle n_e^{eff} \right\rangle = \frac{1}{d}\int_0^d \frac{n_e n_o \, dz}{\sqrt{n_e^2 \sin^2\varphi(z) + n_o^2 \cos^2\varphi(z)}} \tag{1}$$

where d is the effective thickness of the liquid crystal layer, n_e and n_o are extraordinary and ordinary indexes of refraction and $\varphi(z)$ is the angle between the nematic director $\hat{n} = (\cos\varphi(z), 0, \sin\varphi(z))$ and the x-axis.

The extraordinary polarized laser light reads the refractive index and is retarded proportionally to the index changes. When instead of projection of an image onto optically addressed LC spatial light modulato an intensity grating $I(x) = I_0(1 + m\cos(qx))$ is projected then extraordinary polarized light will be diffracted on the so produced refractive index grating. The grating wavevecto $q = 2\pi/\Lambda$ is determined by grating period Λ which in turn depends on wave mixing angle θ. For most of practical cases when grating period is of several microns the diffraction is described within Raman-Nath regime i.e. thin-grating limit is fulfilled. Almost pure phase grating arising in the bulk of liquid crystal layer allows for efficient light diffraction described by:

$$\eta = \left| J_1(\phi) \right|^2 \quad \text{wit} \quad \phi = \frac{2\pi\Delta n_e d}{\lambda} \quad . \tag{2}$$

The maximum expected light diffraction efficienc η in that case can be as high as 34 % what follows from the formula (2) where $J_1(\phi)$ is the Bessel function of the first order. Sinusoidal grating of the form $n_e(x) = n_{0,e} + \Delta n_e \cos(qx - \phi_P)$ where Δn_e is a phase grating amplitude constitutes the simplest hologram. Such type of holograms are studied in most papers devoted to the subject because in such cases interpretation of the results is simplified. However, for practical applications such as optical correlation or holography one deals with complicated light intensity patterns which carry information about 2-D or even 3-D objects. Frequently the illumination level of the spatial light modulator is highl nonuniform and gratings can not be treated as sinusoidal. This causes serious departures from predicted by Eq. (2) efficiency, usually limiting the theoretically predicted values. Only matured photorefractive systems can be used for real time holography where high optical quality, high resolution and sensitivit to light are required. The resolution of the OASLM is only restricted by the defected structure of the nematic LC, but it is typically about 10 - 100 times higher than that of electrically addressed SLM. In grating experiments 100 line pairs/mm were easily achieved. For dynamic purposes the system must be totally reversible and fast responding. In nematic systems the response times are limited to 50 -100 ms whereas in ferroelectric smectics to 100 μs.

3. OPTICAL RETRIEVAL OF BINARY HOLOGRAMS

Computer-generated hologram (CHG) is a vital element in the optical system and it generally relates to a desired pattern or replay field via a Fourier transform. There is no simple way of generating a CHG that generates an arbitrary replay field. To achieve this optimization techniques such as simulated annealing [42] or the genetic algorithm [43] are required. For simple binary phase modulation holograms the simplest way to find out the optimum combination of pixels giving the target replay field $\mathbf{T}$ is a direct binary search (DBS) method. In this technique one starts from a random pixel values hologram and calculates its replay field (Fourier Transform) $\mathbf{H}_0$. Next the difference between $\mathbf{T}$ and $\mathbf{H}_0$ is taken and summed up in order to obtain the first cost function $\mathbf{C}_0$. Then a pixel state is flipped in a random position and the new replay field $\mathbf{H}_1$ is calculated and from the difference of $\mathbf{T}$ and $\mathbf{H}_1$ new cost $\mathbf{C}_1$ is obtained. Fo $\mathbf{C}_0 < \mathbf{C}_1$ the previous pixel flip is rejected and flip back whereas fo $\mathbf{C}_0 > \mathbf{C}_1$ the pixel flip is accepted and $\mathbf{C}_0$ is updated with new cost $\mathbf{C}_1$. The procedure is continued until $|\mathbf{C}_0 - \mathbf{C}_1|$ reaches a minimum value. The simulated annealing uses DBS but includes also a probabilistic evaluation of the cost function which helps to find out more global minima than DBS method. The symmetry of the binary modulation hologram restricts the useful area of the replay field to the upper or lower half plane, as any pattern generated by a hologram will automatically appear as desired as well as rotated about the origin by 180°. Then the maximum efficiency of the binary phase CHG is restricted as the half of the power is wasted. There are advantages in usage of more levels of phase than binary in order to increase efficiency of the hologram and break the symmetry. We not use them to address the OA SLM because of problems with optical qualit of the devices. For the purpose of this article the holograms of simple objects (bitmaps of maximum 50 x 50 pixels) were calculated using a Holomaster 2.0 shareware software.

We constructed and characterized the holographic projection system utilizing the optically addressed liquid crystal spatial light modulator (OA LC SLM) as a holographic medium. For that purpose we used a commerciall available computer controlled multimedia projector with Liquid Crystal Display (LCD) displaying computer generated holograms onto OA LC SLM. This proof-of-principle demonstration is based on projection with incoherent white light of digital binary holograms and their reconstruction with collimated laser beam. The extraordinary polarized laser light diffracts on the holograms and the first Fraunhofer diffraction order forms the real reconstructed image. The optical system used in this work is shown in Fig. 4.
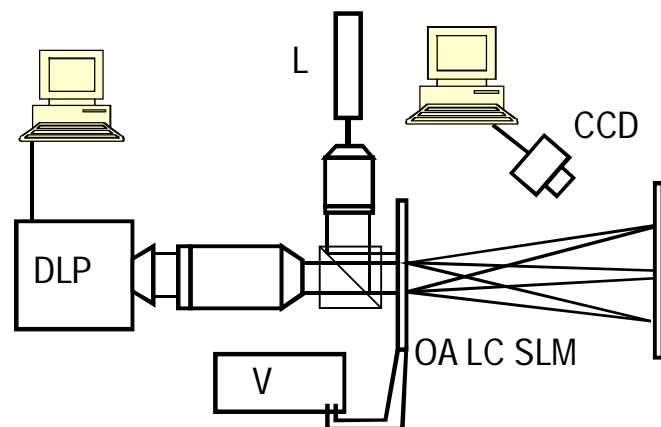

Fig. 4. Digital binary hologram projection system with OA LC SLM. DLP - digital light projector, L -l aser, V - dc voltage supplier, CCD - digital camera.

Spatially modulated light passes through Yashica camera lens system (f = 55 or f = 135 mm) and focuses onto a liquid crystal modulator. To facilitate use of the system the optically addressed liquid crystal spatial light modulator is placed on a micrometer precision moving support. He-Ne laser (cw 5 mW, λ = 543.5 nm) delivers beam, expanded to 1 cm in diameter, which illuminates the binary interferogram optically written on the liquid crystal cell. Clear holographic image is formed at a distance of about 4.7 m. Computed interferogram of the input image which feeds the multimedia

projector is also seen on the monitor and can be changed at video rate. The physical sizes of the binary holograms illuminated onto the OA LC SLM through camera lenses were typically less than 1.5 x 1.5 cm ^{2}. Calculated from diffraction pattern virtual pixel size on OA LC SLM was $\Delta x = 22.2$ μm and $\Delta y = 30.9$ μm. The reconstructed image was recorded by CCD camera from the screen. Image was fine-tuned by an adjustment of SLM position in the optical setup, however performance of the system was dependent on characteristics of the key-element: the photosensitive OA LC SLM.

In the recent paper [44] we described optical reconstruction of computer generated binary holograms displayed directly on EA LC SLM (a matrix containing as much as 640 x 480 addressable 24 μm pixels VGA, Kopin, USA). In this article we compare the performance of the commercial EALC SLM with our OA LC SLM (see Fig. 5). The differences between optically reconstructed images and calculated ones can be noticed in resolution and mutual positions of the objects as well as in the presence of the 0-order light scattering (undiffracted reconstruction wave) which is negligent in the calculated images. The zero order spot is seen in the center of the plane. The noise is mostl due to the limited resolution of the SLM and hologram. One may notice that the differences between the performance of EA LC SLM and OA LC SLM speak in favor of optical addressing. Separate pixels as in the target are well seen in far field of reconstructed hologram. In the case of OA SLM much less of light is scattered into higher orde diffractions due to the smoothing property of liquid crystal modulator besides the images are clearer. We have evaluated that nea 80 % of the diffraction energy is coupled into single Fraunhofer diffraction order while for EA LC SLM it was only ~ 30 %. Spatial resolution of our LC panel, as calculated from virtual pixel size, is better than 45 lines per millimete and a limit estimated from grating recording experiments reaches 250 lp/mm. The speckle diamete $\Delta\xi$ (Airy disk) in the plane of the reconstructed image, which limits the resolution, is given by the formula $\Delta\xi = \lambda d / N \Delta x$. Using N = 200 pixels for reconstruction with $\lambda = 543.5$ nm, $\Delta x = 22.2$ μm and $d = 4.7$ m we calculated that $\Delta\xi \approx 0.6$ mm.
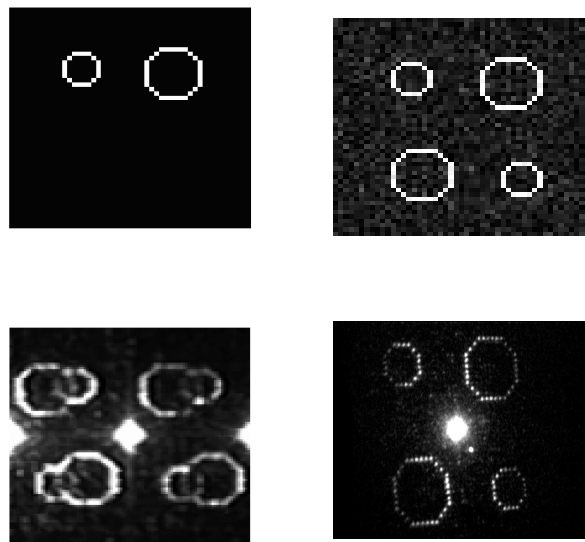

Fig. 5. The diffraction of light on holograms formed in EA (left column) and OA LC SLM's (right column). In the upper row we show an original bitmap and its replica calculated from hologram. Below the hologram reconstructions using EA and OA LC SLM's as the holographic media, respectively are shown.

From separate experiments performed for this panel we have found that measurable phase modulations can be achieved already at light intensities of an order of 10 mW/cm ^{2} for $\lambda = 514.5$ nm. Birefringence of LC extends into IR spectral range therefore these OA LC SLMs can be used in the range 0.5 - 2 μm of reading light wavelength. At least three separate areas of the panel could be simultaneously optically addressed with three different DLP devices and binary holograms read by red, green and blue (RGB) laser light beams. This opens the route to color holographic imaging.

Typically OA LC SLM's required the dc voltage (20 -30 V) and for the best performance voltage was tuned within fe volts range depending on illumination level. Panel response and recovery times to the light pulse depend on man factors and for nematics are: time-on $\approx$ 10-30 ms and time-off $\approx$ 50 - 200 ms. These limits originate from the photoconductive properties of PVK:TNF polymer and ion mobilities in LC. We have checked the dynamic properties of our system by probing the holographic reconstruction at different interferogram writing rates. For that we calculated binary holograms of a letter L and a ball (cf. Fig. 6) and then composed short films in which these holograms were sequentially rotated by a small angle. Rotating interferogram was projected onto OA LCSLM up to frame rate of 30 Hz. Even at maximum rate we could observe a continuous rotation of a letter L in image reconstruction plane without visible residua. No long-term changes of the performance of the OA LC SLM under permanent usage (8-hour video-rate experiment corresponding to 0.864 million completed exposure and erasure cycles) were observed.
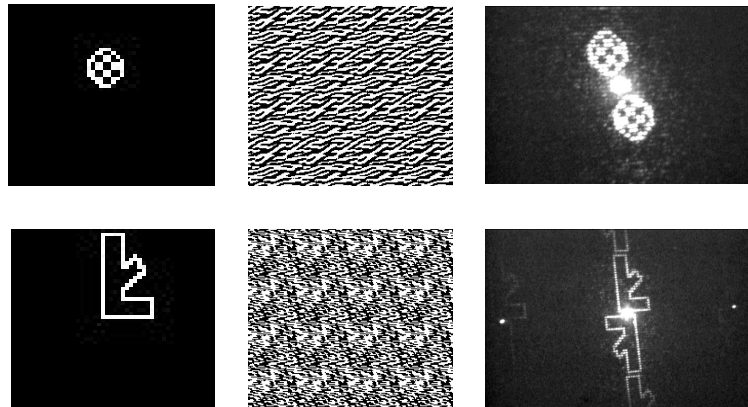

Fig. 6. Examples of bitmaps of 2-D objects (ball and a letter), their computer generated binary holograms that are projected onto OA LC SLM and reconstructed by laser light holograms captured by CCD camera. Besides zero order diffraction the first order spots and images are also seen (cf. reconstructed hologram of L).
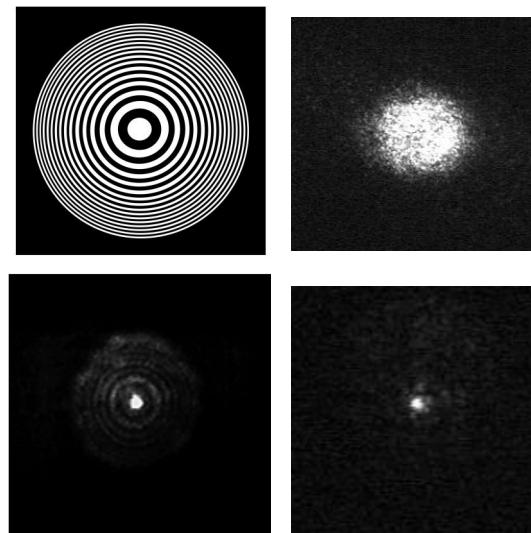

Fig. 7. An example of using OA LC SLM as a pseudo-Fresnel lens. The set of circles (top left) is projected onto LC panel resulting that the collimated beam (top right) is focused to the spot (bottom photographs).

In Fig. 7 we show an example of a computer generated pseudo- Fresnel lens consisting of several concentric rings of different radius and projected on OA LC SLM:

$$f(x,y) = \begin{cases} 1 & \text{for} \quad \cos\left(\pi\dfrac{x^2 + y^2}{\lambda f}\right) > 0 \\ 0 & \text{otherwise} \end{cases}$$

Illumination of such a structure with a collimated laser beam gives the well visible sharp spot at a focal distance. By this we proved that the changeable focus lens can be produced in "all optical" way.

7. CONCLUSIONS

In conclusion we have demonstrated how the liquid crystal panel consisting of the photoconducting layer and the nematic homogenously ordered LC can serve as optically addressed spatial light modulator. The compute generated binary holograms can be projected from a video LCD projector and retrieved optically with the weak powe cw laser beam. The video-rate holographic projection system based on OA LC SLM and operating at low white light intensities and low electric voltage has been described.

8. ACKNOWLEDGMENTS

9. REFERENCES

1. R. L. Powell and K. A. Stetson, "Interferometric vibration analysis by wavefront reconstructions", *J. Opt. Soc. Am.* **55,** 1593-1598, (1965).
2. E. Dufresne, G. Spalding, M. Dearing, S. Sheets and D. Grier, "Computer generated Holographic optical tweezer arrays", *Rev. Sci. Instrum.,* **72**, 1810-1816 (2001).
3. M. L. Huebschman, B. Munjuluri, and H. R. Garner, " Dynamic holographic 3-D image projection", *Optic Express,* **11,** 437-445, (2003).
4. P. Günter, and J.-P. Huignard J.-P. (eds.), *Photorefractive Materials and their Applications*, Vols. 1 and 2, Springer Verlag, Berlin, 1988.
5. S. Ducharme, J. C. Scott, R. J. Twieg and W.E. Moerner, *Phys. Rev. Lett.,* **66**, 1846-1848 (1991).
6. M. Liphardt, A. Goonesekera, B.E. Jones, S. Ducharme, J.M. Takacs, and L. Zhang, „High-performance photorefractive polymers", *Science*, **263**, 367-369 (1994).
7. K. Meerholz, B.L. Volodin, Sandalphon, B. Kippelen, and N. Peyghambarian, „A photorefractive polymer with high optical gain and diffraction efficiency near 100%", *Nature* **371**, 497-499 (1994).
8. M.E. Orczyk, J. Zieba, and P.N. Prasad, „Fast photorefractive effect in PVK :C_{60}:DEANST polymer composite", *J. Phys. Chem.* **98**, 8699-8704 (1994).
9. I.-C. Khoo, *Liquid Crystals Physical Properties and Nonlinear Optical Phenomena*, J. Wiley, New York, 1995.
10. I. Jánossy, A.D. Lloyd, and B.S. Wherrett, „Anomalous optical Freedericksz transition in an absorbing liquid crystal", *Mol. Cryst. Liq. Cryst.* **179**, 1 -12 (1990).
11. I.-C. Khoo, H. Li, and Y. Liang, „Optically induced extraordinarily large negative orientational nonlinearity in dye-doped liquid crystal", *IEEE J. Quant. Electron.* **29**, 1444-1447 (1993).
12. A.G. Chen, and D.J. Brady, „Real-time holography in azo-dye-doped liquid crystals", *Opt. Letters,* **17,** 441-443 (1992).

13. E.V. Rudenko, and A.V. Sukhov, „Optically induced space charge field in nematics and orientational nonlinearity", *JETP (in Russian), ***105**, 1621-1634 (1994).

14. S. Bartkiewicz, A. Miniewicz, A. Januszko, and J. Parka, „Dye-doped liquid crystal composite for real-time holography , *Pure and Applied Optics*, **5,** 799-809 (1996).

15. F. Simoni, *Nonlinear optical properties of liquid crystals and polymer dispersed liquid crystals,* World Scientific, New Jersey, 1997.

16. L. Bouteiller and P. Le Barney, Liq. Cryst. **21**, 157 (1996).

17. C.A. Guymon, E.N. Hoggan, D.M. Walba, N.A. Clark, and C.N. Bowman, Liq. Cryst. **19**, 719 (1995).

18. C.V. Rajaram, S.D. Hudson, and L.C. Chien, Chem. Mater. **7**, 2300 (1995).

19. G.P. Wiederrecht and M.R. Wasielewski, J. Nonl. Opt. Phys. Mater **8**, 107 (1999).

20. T. Todorov, L. Nikolaeva and N. Tomova, Polarization Holography. A New High-Efficiency Organic Material With Reversible Photoinduced Birefringence, Appl. Optics, 23, 4309.(1984).

21. L. M. Blinov, M. V. Kozlovsky and G. Cipparone, Photochromism and Holographic Grating Recording on a Chiral Side-Chain Liquid Crystalline Copolymer Containing Azobenzene Chromophores, Chem. Phys., 245, 473 (1999).

23. R. A. Lessard, C. Lafond, A. Tork, F. Boudreault, T. Galstyan, M. Bolte, A. Ritcey and I. Petkov, Photochromic Materials in Holography, in Multiphoton and Light Driven Multielectron Processes in Organics: New Phenomena, Materials and Application, F. Kajzar and M. V. Agranovich Eds, Kluwer Academic Publishers, Dordrecht, 2000, pp 237-248

24. X. Meng, A. Natahnson C. Barett and P. Rochon, Azo Polymers for Reversible Optical Storage. Cooperative Motion of Polar Side Groups in Amorphous Polymers, Macromolecules, **29**, 946-52 (1996).

25. U. Schnars and W. P. O. Jüptner,"Digital recording and numerical reconstruction of holograms", *Meas. Sci. Technol., ***13,** R85-R101 (2002).

26. W. H. Lee,"Computer-generated holograms: techniques and applications", *Prog. Opt.* **16,** 120-232, (1978).

27. O. Bryngdahl and F. Wyrowski, "Digital holography – computer generated holograms", *Prog. Opt.* **28,** 1-86, (1990).

28. M. Sutkowski and M. Kujawinska, "Application of liquid crystals (LC) fo optoelectronic reconstruction of digitally stored holograms", *Optics&Lasers in Engineering*, **33,** 191-203, (2000).

29. T. Hast, M. Schonleber, H. J. Tiziani, "Computer-generated holograms from 3D-objects written on twisted-nematic liquid crystal displays", *Opt. Commun.,* **140** 299-304, (1997).

30. D. V. Wick, T. Martinez, J. M. Wilkes and M. T. Gruneisen, "Developement of a novel liquid crystal spatial light modulator for real-time holography", *Proc. SPIE,* **3475,** 42- 48, (1998).

31. [9] T. Ito, T. Shimobaba, H. Godo, M. Hoiruchi, "Holographic reconstruction with a 10μm pixel-pitch reflective liquid-crystal display by use of a light-emitting diode reference light", *Opt. Lett.,* **27,** 1406-1409 (2002).

32. T. Kreis, P. Aswendt, R. Hofling, " Hologram reconstruction using a digital micromirror device", *Opt. Eng.,* **40,** 926-929, (2001).

33. R. C. Jones, *J. Opt. Soc. Am.* **32**, 486 (1942).

34. I. Jánossy and A. D. Lloyd, "Low-power optical reorientation in dyed nematics", *Mol. Cryst. Liq. Cryst.* **203,** 77-84, (1991).

35. I.-C. Khoo, H. Li and Y. Liang," Optically induced extraordinarily large negative orientational nonlinearity in dye-doped liquid crystal", *IEEE J. Quant. Electron.* **29,** 1444-1447, (1993).

36. W. M. Gibbons, P. J. Shannon, S.-T. Sun and B. J. Swetlin, "Surface-mediated alignment of nematic liquid crystals with polarized light", *Nature* **351,** 49-50, (1991).

37. A. Miniewicz, S. Bartkiewicz, W. Turalski, A. Januszko, „Dye-doped liquid crystals for real-time holography", in R.W. Munn, A. Miniewicz and B. Kuchta (eds.), *Electrical and Related Properties of Organic Solids*, NATO ASI Series, **3/24**, Kluwer Academic Publishers, Dordrecht, pp. 323-337,1997.

38. F. Simoni, O. Francescangeli, "Effects of light on molecular orientation of liquid crystals", *J. Phys. Condens. Mater,* **11**, R439-R487 (1999).

39. K. Komorowska, A. Miniewicz and J. Parka, " Holographic grating recording in large area photoconducting liquid crystal panels", *Synth. Metals*, **109,** 189-193, (2000).

40. F. Kajzar, S. Bartkiewicz and A. Miniewicz," Optical amplification with high gain in hybrid polymer-liquid crystal structures", *Appl. Phys. Lett*. **74,** 2924-2926 (1999).
41. L. Onsager, *Phys. Rev.*, **54**, 554 (1938)
42. M. P. Dames, R. J. Dowling, P. McKee, D. Wood, *Appl. Opt.* **30**, 2685-2691 (1991)
43. U. Mahlab, J. Shamir, H. J. Caulfield, *Opt. Lett.* **16**, 648-650 (1991)
44. A. Miniewicz, A. Gniewek, J. Parka,"Liquid crystals for photonic applications", *Opt. Mater.* 2**1,** 605-610, (2002).